

Effects of van der Waals Interactions in the Adsorption of Isooctane and Ethanol on Fe(100) Surfaces

Pedro O. Bedolla,^{*,†,‡} Gregor Feldbauer,^{†,‡} Michael Wolloch,^{†,‡} Stefan J. Eder,[‡]
Nicole Dörr,[‡] Peter Mohn,[†] Josef Redinger,[†] and András Vernes^{†,‡}

*Institute of Applied Physics, Vienna University of Technology, Wiedner Hauptstraße 8-10/134,
1040 Vienna, Austria, and Austrian Center of Competence for Tribology (AC2T research GmbH),
Viktor-Kaplan-Straße 2, 2700 Wiener Neustadt, Austria*

E-mail: pb@cms.tuwien.ac.at

Abstract

Van der Waals (vdW) forces play a fundamental role in the structure and behavior of diverse systems. Thanks to development of functionals that include non-local correlation, it is possible to study the effects of vdW interactions in systems of industrial and tribological interest. Here we simulated within the framework of density functional theory (DFT) the adsorption of isooctane (2,2,4-trimethylpentane) and ethanol on a Fe(100) surface, employing various exchange-correlation functionals to take vdW forces into account. In particular, this paper discusses the effect of vdW forces on the magnitude of adsorption energies, equilibrium geometries and their role in the binding mechanism. According to our calculations, vdW interactions increase the adsorption energies and reduce the equilibrium distances. Nevertheless, they do not influence the spatial configuration of the adsorbed molecules. Their effect on the electronic density is a non-isotropic, delocalized accumulation of charge between the molecule and the slab. In conclusion, vdW forces are essential for the adsorption of isooctane and ethanol on a bcc Fe(100) surface.

Introduction

With a universal presence in all molecules and solids, van der Waals forces (vdW) are important interactions to consider in the study of matter.^{1–3} Although weak in comparison to chemical bonds, their long range nature and their collective effect play a decisive role in the structure of molecules and their interaction with surfaces.^{4–7} Nevertheless, their description from first principles has proven to be challenging. Most of the common theoretical methods, such as the density functional theory (DFT), fail to describe them properly. Typically, the commonly used generalized gradient approximation (GGA) underestimates the binding energies and overestimates the equilibrium distances in various physisorbed systems, while the ones calculated within the local density approximation (LDA) are closer to the experiment. However, this better agreement is fortuitous since the exponential decline of the LDA interaction cannot account for the polynomial long-range behaviour of the vdW interactions.^{8,9}

Over the last decade, several approximations have been proposed^{10–39} to take dispersion into account. The most sophisticated methods aim to treat dispersion beyond the pairwise approximation by considering collective excitations. The many-body dispersion approach^{24,25} is one of these models that uses coupled dipoles. The

^{*}To whom correspondence should be addressed

[†]Vienna University of Technology

[‡]AC2T research GmbH

dispersion interaction is obtained from shifts in the frequencies of harmonic oscillators that occupy the atomic positions, as the interaction between them is activated. Although promising, it is challenging to get accurate relations between atoms and oscillator models.⁴⁰ Another model that includes the vdW energy accurately is the random phase approximation,^{27,29–31} combined with the adiabatic connection and fluctuation dissipation theorem.^{26,28} The computational cost of this method limits it at present however, to small systems commonly used as benchmarks. Other models have been proposed that consider dispersion to be pairwise additive but they are otherwise independent of any external input parameters, such as VV10,³⁸ the local response dispersion approach,^{13,14} and the van der Waals density functional (vdW-DF).¹⁰ Klimeš and co-workers^{41,42} proposed a series of optimized functionals within the framework of DFT based on the vdW-DF, which have proven to be among the most accurate in this class of models. Furthermore, the vdW-DF and its optimized versions have been implemented in extensively distributed DFT codes and applied to a wide range of systems including dimers,⁴¹ soft layered materials,⁹ organic molecules adsorbed on graphite,^{43,44} as well as graphene and noble gases on metals,^{8,45,46} among others. These works showed the advantages and disadvantages of these methods and consequently, increased their reliability on subsequent applications.

Of special interest for technological purposes are the interactions between organic molecules and metallic surfaces. The effect of non-local forces have been previously investigated in the adsorption process occurring in promising candidates for opto-electronic devices, including thiophene on Cu(110)⁴⁷ and benzene, along with related compounds, on several transition metals.^{48,49} The influence of dispersion forces has also been studied in the adsorption of *n*-butane on copper and gold surfaces,⁵⁰ which are considered prototypes of typical weak physisorption systems. However, in many industrial applications the metallic surfaces are iron-based alloys. Moreover, the involved molecules may have larger size, be branched, or contain other types of functional groups, as in the case of fuels and lubricants as well as their base fluids and additives. The usefulness of these com-

pounds strongly depends on the interacting forces at the molecule-surface interface, since they play an important role in the tribological behaviour, i.e., low friction and low wear are the most desired requirements for their application.

Recent work in the field of fuel tribology using molecular dynamics (MD) simulations covered the stability of monolayers of stearic acid adsorbed onto nano-rough iron surfaces during shearing^{51,52} or the frictional performance of fuel additives.^{53,54} On the microscale, a joint numerical approach combining the finite-element method and the boundary-element method (FEM-BEM) has been employed to simulate wear processes in a diesel fuel lubricated sliding contact.⁵⁵ However, none of these nano- and microtribological simulations using MD or FEM-BEM explicitly considered the adsorption process as an initial step towards the lubricity of surface-active species. Moreover, the knowledge of the adsorption behavior of ethanol is a crucial preliminary step for a better description of the effectiveness of additives in fuels containing bio-components, i.e. substances with considerably higher polarity in comparison with conventional aliphatic and aromatic fuel components.

Last year, Tereshchuk and Da Silva⁵⁶ studied the adsorption of ethanol and water on several transition-metal surfaces, including Fe(110). Although the reported adsorption energies calculated with vdW corrections are notably different from the corresponding GGA results, the vdW correction applied in that study belongs to a class of empirical approaches which are computationally efficient but, overall, less accurate than other available approaches to take vdW into account.⁴⁰ Thus, a comparison with a method independent of external input parameters is desirable to validate the accuracy of the calculations. Furthermore, a detailed insight into the adsorption mechanism and the influence of the surface termination is required for a better description of these systems. To study the effects of vdW interactions in the adsorption process of molecules and surfaces of industrial and tribological interest, we simulated via first principles calculations the adsorption of isooctane (2,2,4-trimethylpentane) and ethanol on a bcc Fe(100) surface employing various GGA and vdW functionals. These adsorbates were selected be-

cause isooctane is a representative aliphatic gasoline compound and ethanol can be found—besides gasoline—in many relevant products. Additionally, some properties differ remarkably in these molecules, such as the chemical polarity, polarizability and chemical reactivity, and it is therefore possible to investigate their influence on the adsorption process. This paper describes the magnitude of adsorption energies calculated with a rigorous treatment of non-local interactions as well as the influence of vdW forces on equilibrium geometries and their role in the binding mechanism.

Computational details

To study the adsorption energies and equilibrium distances, we carried out spin-polarized first-principles calculations within the framework of DFT.⁵⁷ The Vienna Ab-initio Simulation Package (VASP)^{59–64} was used to perform the required computations. VASP produces an iterative solution of the Kohn-Sham equations within a plane-wave basis, employing periodic boundary conditions. The projector augmented wave (PAW) method⁵⁸ was applied to describe the interaction between the core and the valence electrons.

We considered various approximations to the exchange and correlation functionals. Initially, we tested two functionals constructed in the generalized gradient approximation (GGA): the Perdew, Burke, and Ernzerhof (PBE)^{65,66} and its revised version (revPBE).⁶⁷ These functionals differ only in one parameter of the exchange term, κ , changed from 0.804 in PBE to 1.245 in revPBE and both have been extensively applied in physics and chemistry. In a second step, we employed the vdW density functional (vdW-DF) by Dion et al.,¹⁰

$$E_{xc}^{vdW-DF}[n] = E_{revPBE(x)}[n] + E_{LDA(c)}[n] + E_{nl(c)}[n], \quad (1)$$

where $E_{revPBE(x)}[n]$ is the exchange energy obtained with the revPBE functional, $E_{LDA(c)}[n]$ is an LDA correlation and $E_{nl(c)}[n]$ is a non-local correlation term which approximates the vdW interactions. We also considered the optimized Becke86⁶⁸ van der Waals (optB86b-vdW) functional introduced by Klimeš et al.,^{41,42}

$$E_{xc}^{optB86b-vdW}[n] = E_{optB86b(x)}[n] + E_{LDA(c)}[n] + E_{nl(c)}[n], \quad (2)$$

where a reparametrized version of the Becke86 exchange functional replaces the revPBE exchange used in equation (1). Among the two functionals described in equations (1) and (2), the optB86b-vdW is generally more accurate,⁴² and the results obtained with it should be preferred as reference. However, we apply the vdW-DF to analyze the effects of non-local correlation, since we can subtract the contributions of the other terms by introducing a revPBE+LDA functional,

$$E_{xc}^{revPBE+LDA}[n] = E_{revPBE(x)}[n] + E_{LDA(c)}[n], \quad (3)$$

which involves terms that have been tested and applied in a wide range of materials and whose behaviour, in contrast to the exchange term in equation (2), is well known.

To model our systems, we constructed a supercell consisting of a body-centered cubic (bcc) iron slab and a molecule placed on top of it. Ten layers of atoms were included in the slab, each one containing 25 iron atoms. The vacuum spacing in the z -direction of repeated cells was 29.73 Å. The z axis is parallel to the long axis of the simulation cell and starts at the bottom layer of the iron slab. This set-up accurately models a bcc Fe(100) surface and avoids molecule-molecule and slab-slab interactions, as well as the need to include dipole corrections. The lattice parameter of 2.83 Å used to construct the iron slab was obtained from a bulk calculation for bcc iron, where the calculation parameters were chosen to keep the accuracy consistent with the rest of the computations. This value is in good agreement with the experimental lattice constant of 2.86 Å.⁷¹

To ensure sufficiently accurate total energies and forces, we carefully selected and tested our calculation parameters. The total energies were converged to 10^{-6} eV and a cut-off energy of 400 eV was applied for the plane-wave basis set. The k -space integrations were performed using a $2 \times 2 \times 1$ Monkhorst-Pack mesh,^{69,70} whereas the tetrahedron method with Blöchl corrections was employed for the static calculations and a Gaussian smearing with a width of 0.2 eV for the relaxations. The conjugate gradient algorithm was used to relax the structures, allowing the ions to move until an energy convergence criterion of 10^{-5} eV was fulfilled.

To find the equilibrium structures, we calculated the total energies of varied spatial configurations followed by a relaxation of the most stable one. Various adsorption sites, slab-molecule distances and molecule orientations were analyzed to obtain a better starting guess for the relaxations. During relaxations, the ions in the top four layers of the slab and the ones constituting the molecule were allowed to move in all directions, while the atoms in the remaining layers of the slab were kept fixed to simulate the bulk properties.

We calculated the potential energy curves by varying the distance between the molecule and iron slab, and subsequently computing the total energy of the resulting system via static calculations. The starting geometry for the displacements was the equilibrium structure relaxed with the corresponding functional. The separation between the molecule and the slab (d) was defined as the vertical distance between the atom with the lowest z coordinate in the molecule and the iron atom closest in distance to it. The equilibrium distance was considered to be the separation (as defined above) between the molecule and the slab that minimizes the energy of the system. We stress that this distance is obtained from a finite set of energy points calculated for various values of d and therefore, its accuracy depends on the step size between those values.

Results and discussion

Neither the orientation nor the adsorption site of isooctane and ethanol is influenced by the non-local correlation. Initially, the preferred adsorption configurations were calculated within the GGA approximation. After including non-local interactions in our calculations via the optB86b-vdW functional, a second relaxation did not significantly change the geometry of this configuration. The largest variations in bond lengths were of the order of 10^{-3} Å and in angles, the variations were of the order of 10^{-3} degrees. In the most energetically favorable orientation, the carbon atoms of the isooctane molecule are close to the top and hollow sites of the iron slab (figure 1). The energies of several other orientations differ by only around 20 meV per supercell, and for this reason

no orientation is particularly favored at room temperature, where the thermal energy $k_B T = 25$ meV. Similarly, in the adsorption of ethanol several orientations of the molecule are possible. In this case, however, the hydroxyl group always orients itself towards the slab in all low-energy configurations (figure 2). The plotted geometry differs to the one reported by Tereshchuk and Da Silva⁵⁶ for ethanol adsorbed on the Fe(110) surface only by the C-C bond, which is almost perpendicular to the surface. Our calculated small energy difference of 3 meV between these two configurations indicates that both can coexist at room temperature and that the surface termination does not influence the orientation of the adsorbed molecule. The energy hierarchy of all PBE-structures did not change when it was recalculated with optB86b-vdW to take non-local forces into account.

Non-local interactions increase the adsorption energy of isooctane on a bcc Fe(100) surface and reduce the equilibrium distance (table 1). The absolute value of the adsorption energy calculated with the optB86b-vdW functional is more than 12 times larger than the one calculated with the PBE functional, while the distance between the slab and the molecule, when in equilibrium, is reduced by 1.00 Å (figure 3). To investigate the contribution of the non-local correlation to this increment, we compared the adsorption energies calculated with the vdW-DF and the revPBE+LDA functionals. The resulting energy difference is then 418 meV (figure 3). Since this difference accounts for 95.8% of the adsorption energy calculated with the vdW-DF functional, the variation can now be unambiguously attributed to the dispersion forces. By the same reasoning, the decrease in the binding distance of 1.50 Å can also be associated with non-local interactions.

As a result of the dispersion forces, the non-local correlation between electrons induces the change in the adsorption energy. The equilibrium distance is mainly determined by a balance between the long-range attractive vdW forces and the short-range Pauli repulsion. When the isooctane molecule approaches the iron slab, the Pauli repulsion causes a redistribution of the charge density, particularly among the d-orbitals of the iron ions. No charge is transferred between the molecule and the iron slab during this process. The overlapping



Figure 1: Equilibrium adsorption geometry of an isooctane molecule on a bcc Fe(100) surface. The top, bridge and hollow positions are indicated by a circle, triangle and square, respectively.

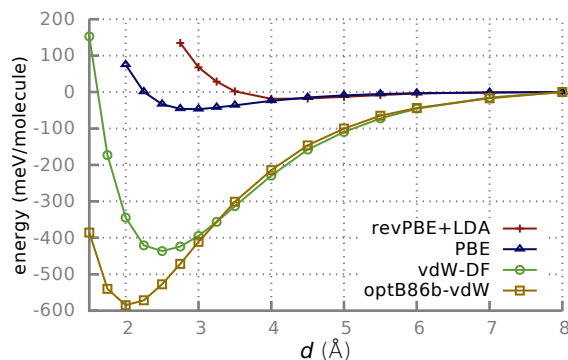


Figure 3: Calculated adsorption energy of an isooctane molecule on the bcc Fe(100) surface as a function of the vertical distance for the PBE, revPBE+LDA, vdW-DF and optB86b-vdW exchange-correlation potentials.

between the wave functions of the molecule and the slab accounts for the movement of the electrons to higher energy states, increasing the total energy of the system. This effect is weaker when a proper description of non-local interactions is considered, because the non-local correlations reduce

the electron-electron repulsion (figure 4). This allows the isooctane molecule to reach a shorter equilibrium distance, where the magnitude of the attractive forces is larger and, consequently, the binding energy increases. The calculated equilibrium distance is also affected by the choice of the vdW density functional, since the Pauli repulsion gives rise to exchange interactions and these functionals differ in the description of the exchange energy. For instance, the difference between the binding distance calculated with the optB86b-vdW functional and the one calculated with the vdW-DF is 0.50 Å.

As in the case of isooctane, the non-local correlation enhances the binding energy between the adsorbed ethanol molecule and the bcc Fe(100) surface and reduces the equilibrium distance (table 1). The adsorption energy calculated with the optB86b-vdW functional is only two times larger than the one calculated with the PBE functional, and the equilibrium separation is 2.00 Å in both cases (figure 8). This difference is remarkably



Figure 2: Equilibrium adsorption geometry of an ethanol molecule on a bcc Fe(100) surface. The top, bridge and hollow positions are indicated by a circle, triangle and square, respectively.

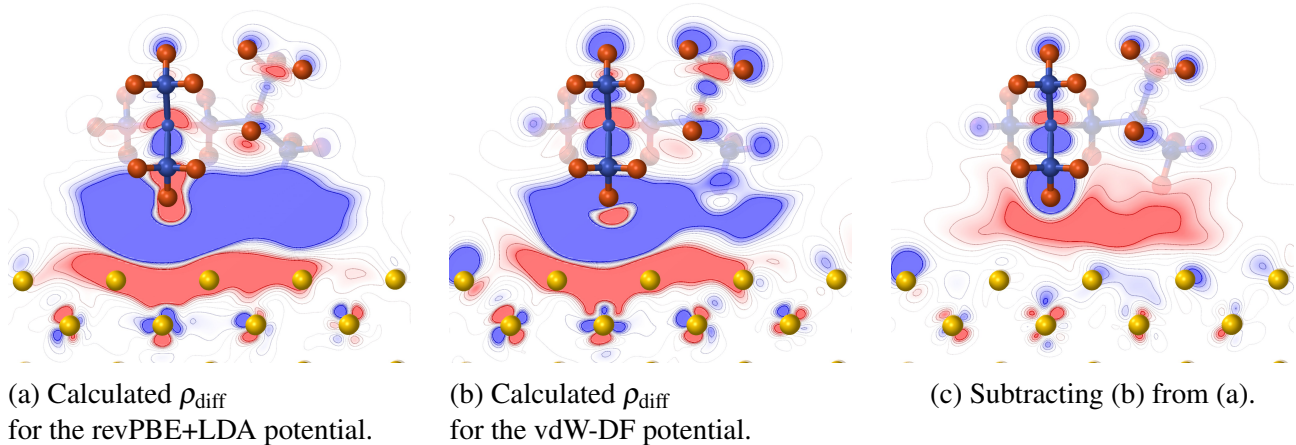


Figure 4: Charge density difference (ρ_{diff}) of isooctane adsorbed on the bcc Fe(100) surface at $d = 2.00$ Å. The charge density difference is defined as $\rho_{\text{diff}} = \rho - (\rho_{\text{isooctane}} + \rho_{\text{Fe}(100)})$ where ρ denotes the charge density of isooctane adsorbed on Fe(100), while $\rho_{\text{isooctane}}$ and $\rho_{\text{Fe}(100)}$ represent the charge densities of the isolated molecule and the clean Fe(100) surface, respectively. The charge density difference is plotted in a plane perpendicular to the surface for values between -5×10^{-4} (solid blue, deficit) and 5×10^{-4} (solid red, accumulation) electrons/Å³.

smaller than the one in the adsorption of isooctane and can be caused either by the involvement of other forces in the binding mechanism or by an artifact, as in the LDA functional. To investigate these possibilities, the effect of the long-range interactions is extracted by comparing calculations with the vdW-DF functional to calculations with revPBE+LDA, as previously described. The contribution to the adsorption energy which can be attributed to the dispersion forces is 95% (figure 8). Although this shows a significant contribution of the non-local interactions to the binding mechanism, the difference of 278 meV between the adsorption energies calculated with the vdW-DF and the optB86b-vdW functional needs to be investigated before discarding the contribution of other forces to the adsorption energy.

The non-local interactions contribute to the binding process of isooctane by inducing an accumulation of charge between the iron surface and the adsorbed molecule. Thonhauser et al.⁷² showed the nature of the vdW bonds in the argon dimer by comparing the induced electron density between two calculations that differ in the inclusion of a term corresponding to the non-local correlation energy. This was justified because, as a consequence of the rapid electronic motions, the nuclei are immune to the fluctuations of the

Table 1: Adsorption energies and equilibrium distances calculated with various exchange-correlation functionals

Functional	Ads. energy (meV)		Eq. distance (Å) ¹	
	Isooctane	Ethanol	Isooctane	Ethanol
PBE	47	384	3.00	2.00
revPBE+LDA	18	26	4.00	4.00
revPBE	-	144	-	2.25
optB86b	585	795	2.00	2.00
vdW-DF	436	517	2.50	2.25

¹ As previously mentioned, the equilibrium distance is determined from a finite set of structures with fixed values of d , with a stepsize of 0.25 Å or smaller.

Coulomb forces and therefore, the charge distribution must deform to produce the required forces on the nuclei by classical Coulomb interactions alone. These forces can be calculated, as shown by Hellman⁷³ and Feynman,⁷⁴ by exploiting the stationary property of the energy with respect to variations in the wave function. Our calculations with the vdW-DF and revPBE+LDA functional allow for a similar treatment of the molecules considered in this work. In the adsorption of isooctane, the non-local interactions cause a non-isotropic accumulation of charge in the region between the molecule and the slab (figure 4). The electrostatic forces arising from this charge redistribution are

responsible for the adsorption of isooctane.

In addition to dispersion forces, a weak electrostatic interaction contributes to the adsorption of ethanol on Fe(100). According to a comparison between the results obtained with revPBE+LDA and vdW-DF, the amount of charge that accumulates as a consequence of non-local interactions is larger and extends over a wider area (figure 5). However, in contrast to the case of isooctane, in this system the charge redistributions predicted by these functionals differ considerably. According to the results obtained with the revPBE+LDA functional, in the absence of non-local correlations the Pauli repulsion produces a region of deficit of charge between the surface and the molecule and displaces the electronic density above the molecule. This considerable redistribution of charge (figure 5a) and the small adsorption energy (table 1) calculated with this functional suggest that it is overly repulsive in this system. A similar behavior has been observed before for the revPBE functional (exchange and correlation) in molecules at short separations.⁷⁵ A calculation with the revPBE functional predicts a larger absorption energy (figure 8) but it is, nevertheless, less than half of the one calculated with the PBE functional. Evidently, this system is heavily influenced by the description of the exchange energy, since the only difference between these two functionals lies in the exchange term. The charge redistribution calculated with the PBE functional (figure 6a) resembles the one calculated with vdW

functionals (figures 5b and 6b). Since PBE does not include the effects of non-local correlations, this last result indicates that an important contribution to the binding between the ethanol and the Fe(100) surface cannot be attributed to the dispersion forces alone. Based on previously estimated adsorption energies, it has been proposed that a weak chemisorption is involved in the binding mechanism.⁵⁶ Our calculations, however, do not show a charge transfer large enough to consider the formation of an ionic bond and the analysis of the electron localization function (ELF)^{76,77} do not point to the existence of localized electrons forming a bond between the molecule and the metallic slab (figure 7). The optB86b-vdW functional predicts a lesser amount of charge between the ethanol and the iron slab than the one calculated with PBE, particularly between the hydroxyl group and the closest iron atom to it (figure 6c). Since this effect is accompanied by an increase in the adsorption energy, a weak electrostatic interaction together with the dispersion forces may constitute the main mechanisms contributing to the adsorption. Nevertheless, this comparison does not allow to separate these contributions, since these functionals differ in the exchange term.

The difference in the adsorption process of isooctane and ethanol on a bcc Fe(100) surface can be understood in terms of the polarizability of the molecules and the charge density distribution around the functional group. Clearly, isooctane is

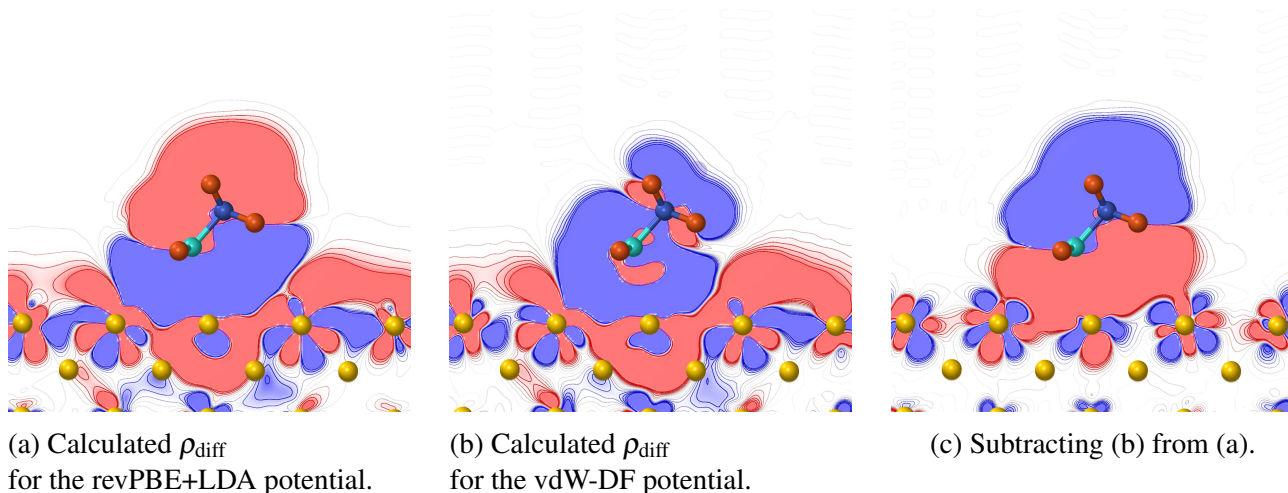


Figure 5: Charge density difference (ρ_{diff}) of ethanol adsorbed on the bcc Fe(100) surface at $d = 2.00$ Å. The charge density difference is defined and plotted in an analogous way to figure 4.

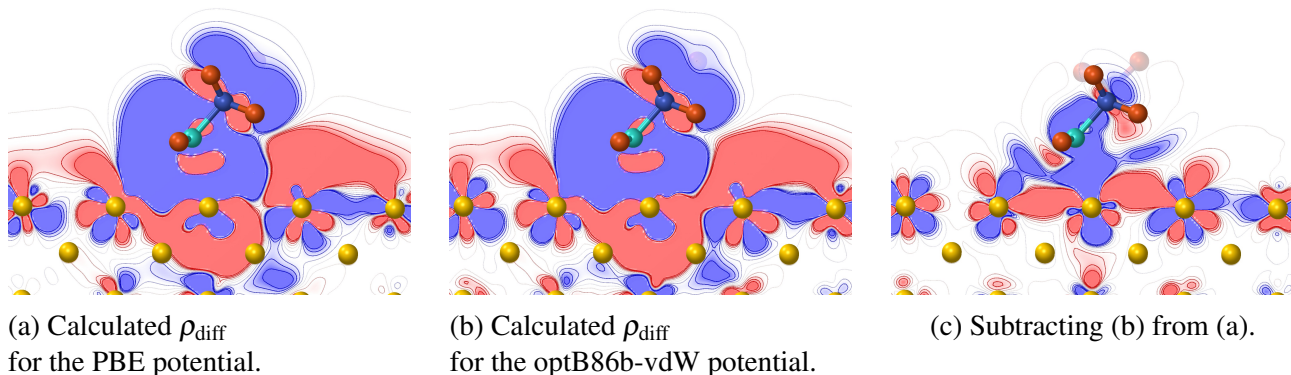


Figure 6: Charge density difference (ρ_{diff}) of ethanol adsorbed on the bcc Fe(100) surface at $d = 2.00$ Å. The charge density difference is defined and plotted in an analogous way to figure 4.

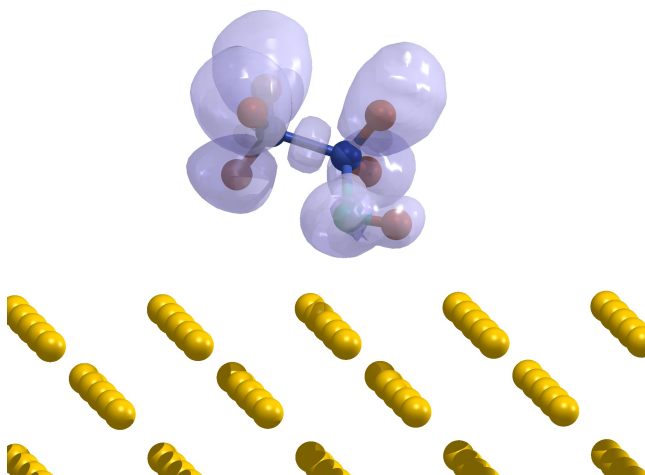


Figure 7: Isosurface at ELF = 0.50 of ethanol adsorbed on Fe(100) at $d = 2.00$ Å calculated with the optB86b functional. Electrons “outside” this isosurface are expected to be delocalized.

expected to be more polarizable than ethanol because of its larger molecular size. Additionally, it is well known that alkanes are among the most polarizable molecules.⁷⁸ Since dispersion forces arise from the formation of instant multipoles, their strength is directly related to the polarizability. Moreover, the absence of a functional group in isooctane leaves dispersion forces as the only possible binding mechanism. On the other hand,

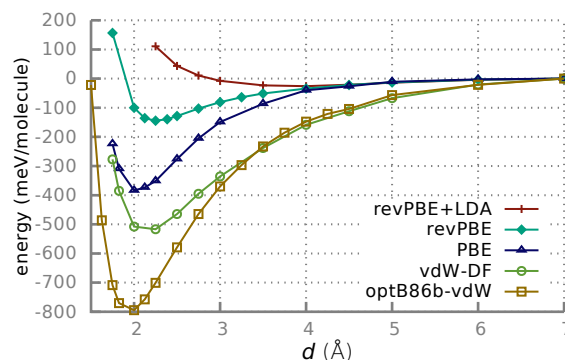


Figure 8: Calculated adsorption energy of an ethanol molecule on the bcc Fe(100) surface as a function of the vertical distance for the PBE, revPBE+LDA, vdW-DF and optB86b-vdW exchange-correlation potentials.

ethanol has a permanent dipole, product of the difference in electronegativity between the hydrogen and the oxygen atom in the hydroxyl group, and non-bonding electrons in the oxygen. During the adsorption process, not only the dispersion forces contribute to the binding but there is also a weak electrostatic interaction between the hydroxyl group and the iron slab, where the charge redistribution leads to the formation of multipoles on the top layer (figures 5 and 6). Consequently, the iron surface binds ethanol stronger than isooctane even though the contribution of the dispersion forces is expected to be weaker than in isooctane.

Summary and outlook

The vdW forces are essential for the adsorption of isooctane and ethanol on a bcc Fe(100) surface. As product of these long-range interactions, the non-local correlation leads to an increase in the adsorption energies and a reduction of the equilibrium distances. Nevertheless, they do not influence the spatial configuration of the adsorbed molecules. Their effect on the electronic density is a non-isotropic accumulation of charge between the molecule and the slab.

Our calculations are a first approach towards a more rigorous treatment of vdW interactions in complex systems and they will contribute, after experimental validation, to the development and improvement of vdW functionals which are independent of external input parameters. We showed the effects of non-local interactions in the electronic density and in the adsorption mechanism. Isooctane binds to the Fe(100) surface via dispersion forces while in ethanol, in addition to the dispersion forces, a weak electrostatic interaction between the hydroxyl group and the iron surface contributes to the binding.

We anticipate that with the continuous increase in computing power, future calculations that consider many-body effects in combination with the work here presented will clarify the relevance of these interactions and contribute to a more accurate analysis of the vdW forces in systems of industrial interest. In particular, the obtained results will aid the fitting of accurate surface–lubricant interaction potentials required for classical MD simulations including numerous organic molecules. These interface potentials usually constitute a considerable uncertainty in any such MD simulation, as they are rarely assumed more advanced than a Lennard-Jones potential parameterized according to desorption data. A detailed knowledge of the interaction energy between molecules and metal surface can therefore greatly boost the precision of large-scale atomistic studies of the thermal, mechanical and structural stability of molecular surface films.

Acknowledgement POB, JR and PM acknowledge support from the Austrian Science Funds (FWF) within the SFB ViCoM F4109-N13 P09.

Part of this work was funded by the Austrian COMET Program (Project K2 XTribology, Grant No. 824187), the ERDF, and the province of Lower Austria (Onlab Project) and was carried out at the “Excellence Centre of Tribology”. The computational results presented have been achieved in part using the Vienna Scientific Cluster (VSC).

References

- (1) Lieb, E. H.; Thirring, W. E. Universal nature of van der Waals forces for Coulomb systems. *Phys. Rev. A* **1986**, *34*, 40–46
- (2) Winterton, R. H. S. Van der Waals forces. *Contemp. Phys.* **1970**, *11*, 559–574
- (3) Butt, H.; Kappl, M. *Surface and Interfacial Forces*; Physics textbook; Wiley, 2009
- (4) Atwood, J.; Steed, J. *Encyclopedia of Supramolecular Chemistry*; Dekker Encyclopedias Series v. 2; M. Dekker, 2004
- (5) Lawley, K. *Advances in Chemical Physics, AB INITIO Methods in Quantum Chemistry II*; Advances in Chemical Physics; Wiley, 2009
- (6) Jortner, J. *Advances in Chemical Physics, Photoselective Chemistry*; Advances in Chemical Physics; Wiley, 2009
- (7) Zeng, H. *Polymer Adhesion, Friction, and Lubrication*; Wiley, 2013
- (8) Mittendorfer, F.; Garhofer, A.; Redinger, J.; Klimeš, J.; Harl, J.; Kresse, G. Graphene on Ni(111): Strong interaction and weak adsorption. *Phys. Rev. B* **2011**, *84*, 201401
- (9) Graziano, G.; Klimeš, J.; Fernandez-Alonso, F.; Michaelides, A. Improved description of soft layered materials with van der Waals density functional theory. *J. Phys.: Condens. Matter* **2012**, *24*, 424216
- (10) Dion, M.; Rydberg, H.; Schröder, E.; Langreth, D. C.; Lundqvist, B. I. Van der Waals Density Functional for General Geometries. *Phys. Rev. Lett.* **2004**, *92*, 246401

- (11) Lee, K.; Murray, E. D.; Kong, L.; Lundqvist, B. I.; Langreth, D. C. Higher-accuracy van der Waals density functional. *Phys. Rev. B* **2010**, *82*, 081101
- (12) Sato, T.; Tsuneda, T.; Hirao, K. Long-range corrected density functional study on weakly bound systems: Balanced descriptions of various types of molecular interactions. *J. Chem. Phys.* **2007**, *126*
- (13) Sato, T.; Nakai, H. Density functional method including weak interactions: Dispersion coefficients based on the local response approximation. *J. Chem. Phys.* **2009**, *131*, 224104
- (14) Sato, T.; Nakai, H. Local response dispersion method. II. Generalized multicenter interactions. *J. Chem. Phys.* **2010**, *133*, 194101
- (15) Grimme, S. Semiempirical GGA-type density functional constructed with a long-range dispersion correction. *J. Comput. Chem.* **2006**, *27*, 1787–1799
- (16) Grimme, S.; Antony, J.; Ehrlich, S.; Krieg, H. A consistent and accurate ab initio parametrization of density functional dispersion correction (DFT-D) for the 94 elements H-Pu. *J. Chem. Phys.* **2010**, *132*
- (17) Grimme, S. Density functional theory with London dispersion corrections. *Comp. Mol. Sci.* **2011**, *1*, 211–228
- (18) Antony, J.; Grimme, S. Density functional theory including dispersion corrections for intermolecular interactions in a large benchmark set of biologically relevant molecules. *Phys. Chem. Chem. Phys.* **2006**, *8*, 5287–5293
- (19) von Lilienfeld, O. A.; Tavernelli, I.; Rothlisberger, U.; Sebastiani, D. Optimization of Effective Atom Centered Potentials for London Dispersion Forces in Density Functional Theory. *Phys. Rev. Lett.* **2004**, *93*, 153004
- (20) von Lilienfeld, A. O.; Tkatchenko, A. Two- and three-body interatomic dispersion energy contributions to binding in molecules and solids. *J. Chem. Phys.* **2010**, *132*, 234109
- (21) Becke, A. D.; Johnson, E. R. Exchange-hole dipole moment and the dispersion interaction revisited. *J. Chem. Phys.* **2007**, *127*
- (22) Tkatchenko, A.; Scheffler, M. Accurate Molecular Van Der Waals Interactions from Ground-State Electron Density and Free-Atom Reference Data. *Phys. Rev. Lett.* **2009**, *102*, 073005
- (23) Tkatchenko, A.; Romaner, L.; Hofmann, O. T.; Zofer, E.; Ambrosch-Draxl, C.; Scheffler, M. Van der Waals Interactions Between Organic Adsorbates and at Organic/Inorganic Interfaces. *MRS Bulletin* **2010**, *35*, 435–442
- (24) Tkatchenko, A.; DiStasio, R. A.; Car, R.; Scheffler, M. Accurate and Efficient Method for Many-Body van der Waals Interactions. *Phys. Rev. Lett.* **2012**, *108*, 236402
- (25) Cole, M. W.; Velegol, D.; Kim, H.-Y.; Lucas, A. A. Nanoscale van der Waals interactions. *Macromol. Symp.* **2009**, *35*, 849–866
- (26) Dobson, J. F.; Dinte, B. P. Constraint Satisfaction in Local and Gradient Susceptibility Approximations: Application to a van der Waals Density Functional. *Phys. Rev. Lett.* **1996**, *76*, 1780–1783
- (27) Furche, F. Molecular tests of the random phase approximation to the exchange-correlation energy functional. *Phys. Rev. B* **2001**, *64*, 195120
- (28) Furche, F.; Van Voorhis, T. Fluctuation-dissipation theorem density-functional theory. *J. Chem. Phys.* **2005**, *122*, 164106
- (29) Ángyán, J. G.; Liu, R.-F.; Toulouse, J.; Jansen, G. correlation energy expressions from the adiabatic-connection fluctuation–dissipation theorem approach. *J. Chem. Theory Comput.* **2011**, *7*, 3116–3130
- (30) Heßelmann, A. Random-phase-approximation correlation method including exchange interactions. *Phys. Rev. A* **2012**, *85*, 012517

- (31) Harl, J.; Kresse, G. Accurate Bulk Properties from Approximate Many-Body Techniques. *Phys. Rev. Lett.* **2009**, *103*, 056401
- (32) Riley, K. E.; Pitoňák, M.; Jurečka, P.; Hobza, P. Stabilization and Structure Calculations for Noncovalent Interactions in Extended Molecular Systems Based on Wave Function and Density Functional Theories. *Chem. Rev.* **2010**, *110*, 5023–5063
- (33) Kannemann, F. O.; Becke, A. D. van der Waals Interactions in Density-Functional Theory: Intermolecular Complexes. *J. Chem. Theory Comput.* **2010**, *6*, 1081–1088
- (34) Steinmann, S. N.; Corminboeuf, C. Comprehensive Benchmarking of a Density-Dependent Dispersion Correction. *J. Chem. Theory Comput.* **2011**, *7*, 3567–3577
- (35) Misquitta, A. J.; Podeszwa, R.; Jeziorski, B.; Szalewicz, K. Intermolecular potentials based on symmetry-adapted perturbation theory with dispersion energies from time-dependent density-functional calculations. *J. Chem. Phys.* **2005**, *123*, 075312
- (36) Johnson, E. R.; Becke, A. D. A post-Hartree–Fock model of intermolecular interactions. *J. Chem. Phys.* **2005**, *123*, 024101
- (37) Silvestrelli, P. L. Van der Waals Interactions in DFT Made Easy by Wannier Functions. *Phys. Rev. Lett.* **2008**, *100*, 053002
- (38) Vydrov, O. A.; Van Voorhis, T. Nonlocal van der Waals density functional: The simpler the better. *J. Chem. Phys.* **2010**, *133*, 244103
- (39) Cooper, V. R.; Kong, L.; Langreth, D. C. Computing dispersion interactions in density functional theory. *Physics Procedia* **2010**, *3*, 1417 – 1430, Proceedings of the 22th Workshop on Computer Simulation Studies in Condensed Matter Physics (CSP 2009)
- (40) Klimeš, J.; Michaelides, A. Perspective: Advances and challenges in treating van der Waals dispersion forces in density functional theory. *J. Chem. Phys.* **2012**, *137*, 120901
- (41) Klimeš, J.; Bowler, D. R.; Michaelides, A. Chemical accuracy for the van der Waals density functional. *J. Phys.: Condens. Matter* **2010**, *22*, 022201
- (42) Klimeš, J.; Bowler, D. R.; Michaelides, A. Van der Waals density functionals applied to solids. *Phys. Rev. B* **2011**, *83*, 195131
- (43) Chakarova-Käck, S. D.; Borck, O.; Schröder, E.; Lundqvist, B. I. Adsorption of phenol on graphite(0001) and α -Al₂O₃(0001): Nature of van der Waals bonds from first-principles calculations. *Phys. Rev. B* **2006**, *74*
- (44) Chakarova-Käck, S. D.; Schröder, E.; Lundqvist, B. I.; Langreth, D. C. Application of van der Waals Density Functional to an Extended System: Adsorption of Benzene and Naphthalene on Graphite. *Phys. Rev. Lett.* **2006**, *96*, 146107
- (45) Vanin, M.; Mortensen, J. J.; Kelkkanen, A. K.; Garcia-Lastra, J. M.; Thygesen, K. S.; Jacobsen, K. W. Graphene on metals: A van der Waals density functional study. *Phys. Rev. B* **2010**, *81*, 081408
- (46) Chen, D.-L.; Al-Saidi, W. A.; Johnson, J. K. Noble gases on metal surfaces: Insights on adsorption site preference. *Phys. Rev. B* **2011**, *84*, 241405
- (47) Sony, P.; Puschnig, P.; Nabok, D.; Ambrosch-Draxl, C. Importance of Van Der Waals Interaction for Organic Molecule-Metal Junctions: Adsorption of Thiophene on Cu(110) as a Prototype. *Phys. Rev. Lett.* **2007**, *99*, 176401
- (48) Liu, W.; Carrasco, J.; Santra, B.; Michaelides, A.; Scheffler, M.; Tkatchenko, A. Benzene adsorbed on metals: Concerted effect of covalency and van der Waals bonding. *Phys. Rev. B* **2012**, *86*, 245405
- (49) Li, G.; Tamblyn, I.; Cooper, V. R.; Gao, H.-J.; Neaton, J. B. Molecular adsorption on metal surfaces with van der Waals density functionals. *Phys. Rev. B* **2012**, *85*, 121409

- (50) Lee, K.; Morikawa, Y.; Langreth, D. C. Adsorption of *n*-butane on Cu(100), Cu(111), Au(111), and Pt(111): Van der Waals density functional study. *Phys. Rev. B* **2010**, *82*, 155461
- (51) Eder, S.; Vernes, A.; Betz, G. Methods and numerical aspects of nanoscopic contact area estimation in atomistic tribological simulations. *Comput. Phys. Commun.* **2014**, *185*, 217–228
- (52) Eder, S.; Vernes, A.; Vorlaufer, G.; Betz, G. Molecular dynamics simulations of mixed lubrication with smooth particle post-processing. *J. Phys.: Condens. Matter* **2011**, *23*, 175004
- (53) Eder, S.; Vernes, A.; Betz, G. On the Derjaguin Offset in Boundary-Lubricated Nanotribological Systems. *Langmuir* **2013**, *29*, 13760–13772
- (54) Vernes, A.; Eder, S.; Vorlaufer, G.; Betz, G. On the three-term kinetic friction law in nanotribological systems. *Faraday Discuss.* **2012**, *156*, 173–196
- (55) Ilincic, S.; Vernes, A.; Vorlaufer, G.; Hunger, H.; Dörr, N.; Franek, F. Numerical estimation of wear in reciprocating tribological experiments. *Proc. Inst. Mech. Eng. J J. Eng. Tribol.* **2013**, *227*, 510–519
- (56) Tereshchuk, P.; Da Silva, J. L. F. Ethanol and Water Adsorption on Close-Packed 3d, 4d, and 5d Transition-Metal Surfaces: A Density Functional Theory Investigation with van der Waals Correction. *J. Phys. Chem. C* **2012**, *116*, 24695–24705
- (57) Kohn, W.; Sham, L. J. Self-consistent equations including exchange and correlation effects. *Phys. Rev.* **1965**, *140*, A1133–A1138
- (58) Blöchl, P. E. Projector augmented wave method. *Phys. Rev. B* **1994**,
- (59) Kresse, G.; Hafner, J. Ab initio molecular dynamics for liquid metals. *Phys. Rev. B* **1993**, *47*, 558
- (60) Kresse, G.; Hafner, J. Norm-Conserving and ultrasoft pseudopotentials for first-row and transition-elements. *J. Phys.: Condens. Matter* **1994**, *6*, 8245
- (61) Kresse, G.; Hafner, J. Ab initio molecular-dynamics simulation of the liquid-metal-amorphous-semiconductor transition in germanium. *Phys. Rev. B* **1994**, *49*, 14251
- (62) Kresse, G.; Furthmüller, J. Efficient iterative schemes for ab initio total-energy calculations using a plane-wave basis set. *Phys. Rev. B* **1996**, *54*, 11169
- (63) Kresse, G.; Furthmüller, J. Efficiency of ab-initio total energy calculations for metals and semiconductors using a plane-wave basis set. *Comput. Mat. Sci.* **1996**, *6*, 15
- (64) Kresse, G.; Joubert, D. From ultrasoft pseudopotentials to the projector augmented wave method. *Phys. Rev. B* **1999**, *59*, 1758
- (65) Perdew, J. P.; Burke, K.; Ernzerhof, M. Generalized gradient approximation made simple. *Phys. Rev. Lett.* **1996**, *77*, 3865–3868
- (66) Perdew, J. P.; Burke, K.; Ernzerhof, M. Erratum: Generalized gradient approximation made simple. *Phys. Rev. Lett.* **1997**, *78*, 1396
- (67) Zhang, Y.; Yang, W. Comment on “Generalized Gradient Approximation Made Simple”. *Phys. Rev. Lett.* **1998**, *80*, 890–890
- (68) Becke, A. D. On the large gradient behavior of the density functional exchange energy. *J. Chem. Phys.* **1986**, *85*
- (69) Monkhorst, H. J.; Pack, J. D. Special points for Brillouin-zone integrations. *Phys. Rev. B* **1976**, *13*, 5188–5192
- (70) Methfessel, M.; Paxton, A. T. High-precision sampling for Brillouin-zone integration in metals. *Phys. Rev. B* **1989**, *40*, 3616–3621
- (71) Wyckoff, R. *Crystal structures*, 2nd ed.; CRYSTAL STRUCTURES, 2ND EDITION Series; Interscience Publishers, 1971

- (72) Thonhauser, T.; Cooper, V. R.; Li, S.; Puzder, A.; Hyldgaard, P.; Langreth, D. C. Van der Waals density functional: Self-consistent potential and the nature of the van der Waals bond. *Phys. Rev. B* **2007**, 76, 125112
- (73) Hellmann, H. *Einführung in die Quantenchemie*; Franz Deuticke, 1937
- (74) Feynman, R. P. Forces in Molecules. *Phys. Rev.* **1939**, 56, 340–343
- (75) Murray, E. D.; Lee, K.; Langreth, D. C. Investigation of Exchange Energy Density Functional Accuracy for Interacting Molecules. *J. Chem. Theory Comput.* **2009**, 5, 2754–2762
- (76) Becke, A.; Edgecombe, K. A simple measure of electron localization in atomic and molecular systems. *J. Chem. Phys.* **1990**, 92, 5397–5403, cited By (since 1996)1672
- (77) Silvi, B.; Savin, A. Classification of chemical bonds based on topological analysis of electron localization functions. *Nature* **1994**, 371, 683–686
- (78) Anslyn, E.; Dougherty, D. *Modern Physical Organic Chemistry*; University Science, 2006